Synthesis of Sphere Packings for Evaluation of Image Segmentation Algorithms

Ramaprasad Kulkarni[1], Marcel G. Schaap[2], Jeffrey J. Rodriguez[1], and Markus Tuller[2]

[1] University of Arizona, Dept. of Electrical and Computer Engineering, Tucson, AZ

[2] University of Arizona, Dept. of Soil, Water and Environmental Science, Tucson, AZ

THE UNIVERSITY OF ARIZONA®

Introduction

- **X-ray CT provides powerful means for characterization and visualization of phase distributions in porous media (see example in Fig. 1). However, selection of appropriate segmentation algorithms for converting fuzzy grayscale images to distinct phases and particularly to test their performance and identify any limitations is challenging, mainly because of the lack of reference data.**
- **To overcome these problems, we first applied Discrete Element Modeling (DEM) to generate realistic sphere packings exhibiting different porosities and particle size distributions. Then lattice Boltzmann (LB) simulations were performed to generate wetting-phase distributions for various saturation levels. Finally, different noise sources and levels that resemble noise introduced during X-ray CT scanning were added to test the applicability and potential failure of four multi-phase segmentation algorithms.**

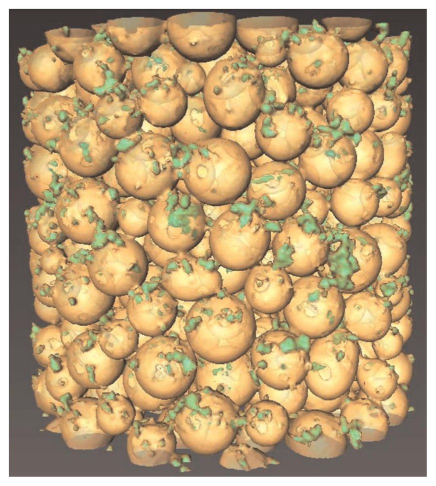

Figure 1: X-ray microtomography imaging of biofilms grown on glass beads (Iltis et al., 2011).

Synthesis of Sphere Packings with DEM

- **Discrete Element Modeling (DEM) can be applied to simulate the motion of particles based on classical mechanics laws considering gravitational, Hertz contact, and frictional forces. While this approach is widely applied in the mining industry to design hopper systems, it can be adapted for simulation of random sphere packings via emulating the pouring of spherical particles into a cylindrical container.**
- **As a preliminary test we generated two sphere packings with distinct particle size distributions and porosities. First, the *ESyS-Particle* open source code was applied to generate distributions of spherical particles with diameters sampled from uniform random distributions for ranges of 0.1 – 0.4 and 0.5 – 1.0 diameter units, respectively. Then the *Yade-DEM* open source software package (*Šmilauer et al., 2010*) was utilized to emulate the pouring of the particles into a cylindrical container of 4 diameter units size (Fig. 2) to generate the two stable sphere packings depicted in Fig. 3. Note that target porosities cannot be defined a priori; only the bounds for the particle sizes may be specified in *ESyS-Particle*.**

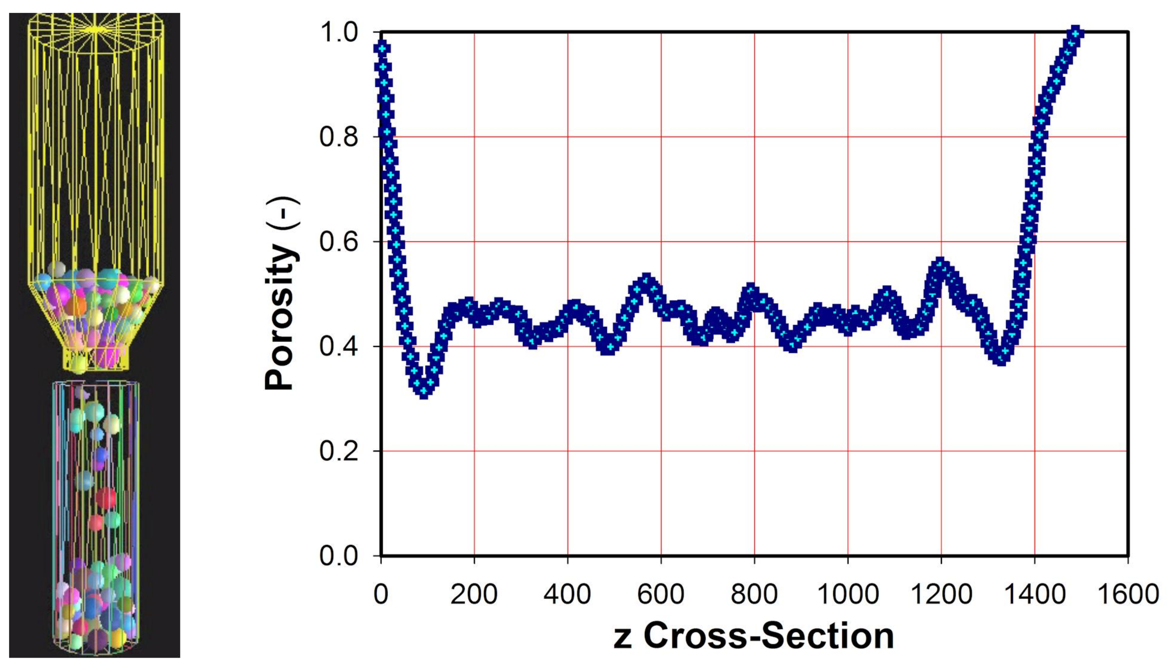

Figure 2: Screen capture of pouring particles of 0.5-1.0 diameter units size range with *Yade-DEM* (left) and porosity plotted along the z-dimension of the cylinder for the same packing (right).

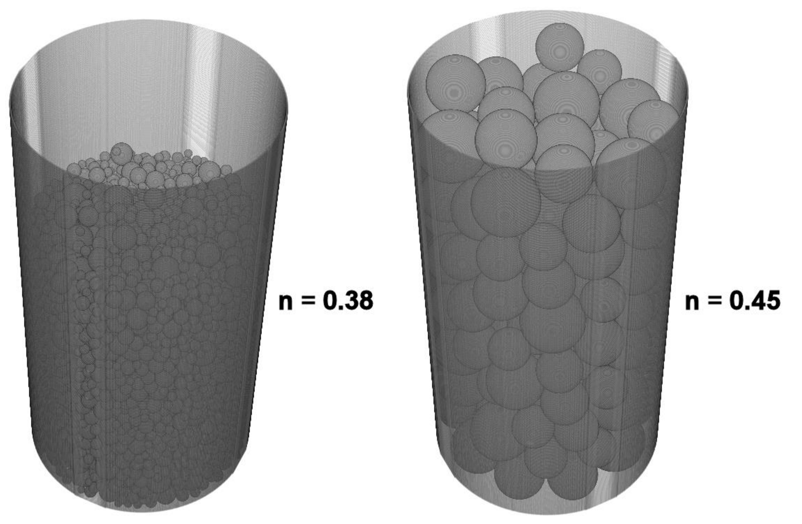

Figure 3: Stable sphere packings with porosities of 0.38 (left) and 0.45 (right) generated with *Yade-DEM*.

Addition of Wetting-Phase with LB Simulations

- **We applied the Shan-Chen multiple component lattice Boltzmann (LB) model (*Schaap et al., 2007*) that allows simulation of miscible and immiscible fluid systems. Interaction between the components (i.e., water and air) allows for fluid separation with one of the components dominating in each phase (major component) and the other being present as a minor component. Fluid separation leads to curved fluid interfaces and the notion of surface tension. Component interactions with the solid phase allow specification of wettability and a fluid-solid contact angle.**
- **The sphere packings generated with *Yade-DEM* were used as boundaries for LB simulations. Pressure boundary conditions were applied to obtain approximate relative wetting-phase saturations of 0.1, 0.5 and 0.9 for both sphere packings (Figs. 4 and 5). Note that the solid-liquid contact angle was set to zero.**

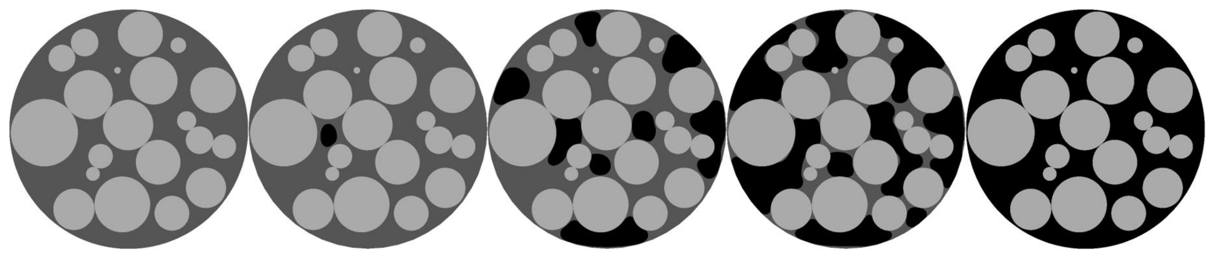

Figure 4: Sample cross-sections with relative wetting-phase saturations of 1.0, 0.9, 0.5, 0.1, and 0.0 (left to right) for the sample with a porosity of 0.45.

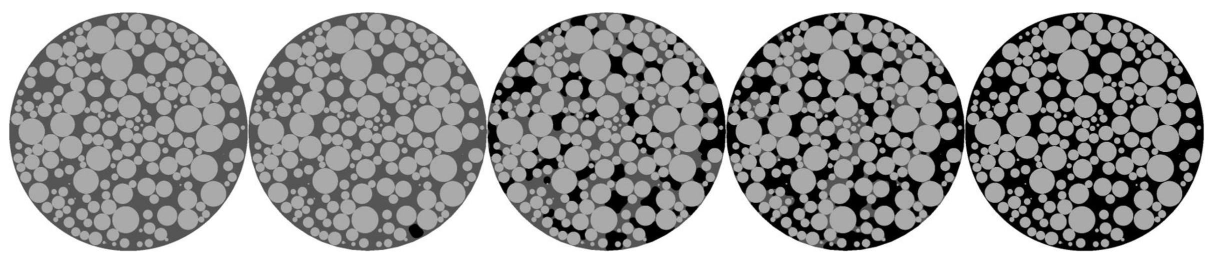

Figure 5: Sample cross-sections with relative wetting-phase saturations of 1.0, 0.9, 0.5, 0.1, and 0.0 (left to right) for the sample with a porosity of 0.38.

Addition of X-ray CT Artifacts

- **For the generated sphere packings with added wetting-phase distributions, which realistically represent three-phase porous systems, the phases are perfectly defined, hence after addition of common artifacts emanating from X-ray CT acquisition they can be employed as reference data to validate binarization as well as multiphase segmentation algorithms.**
- **To generate 3-D grayscale data similar to that obtained with X-ray CT, various known artifacts that potentially affect segmentation and are discussed in *Hsieh* (*2009*) were introduced to the exact three-phase systems. For preliminary tests we added Poisson noise, reduced the contrast between phases, and applied bicubic interpolation to downsample data for mimicking partial volume effects. An example for the sample with 0.45 porosity and a relative wetting-phase saturation of 0.5 is depicted in Fig. 6.**

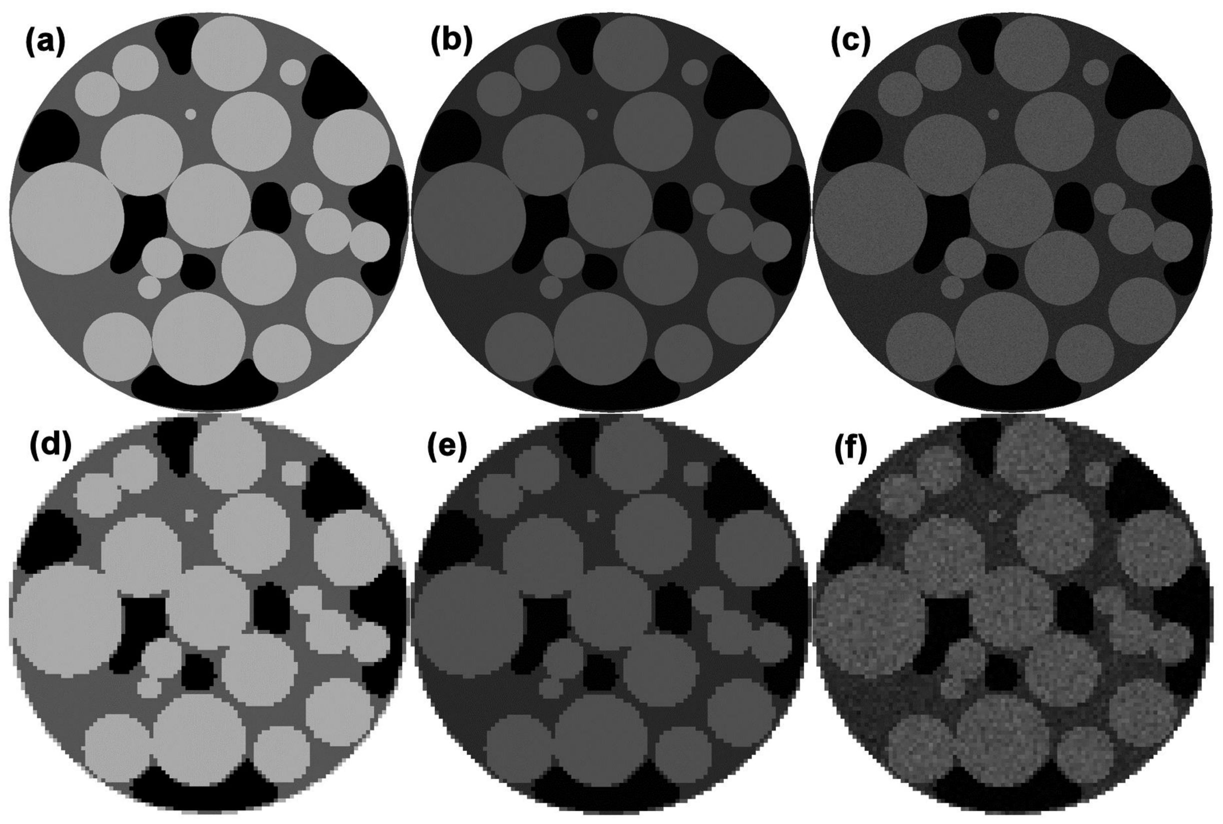

Figure 6: Sample cross-sections for the sample with 0.45 porosity and a relative wetting-phase saturation of 0.5 illustrating the addition of CT acquisition artifacts to the data generated with DEM and LB simulations. Original 800×800 cross-section (a); cross-section after phase contrast reduction (b); and after addition of Poisson noise (c). Similarly, the cross-section after downsampling to 100×100 to mimic partial volume effects (d); after contrast reduction (e); and after addition of Poisson noise (f).

Evaluation of Segmentation Algorithms

- **For this presentation we compared the performance of 4 multiphase segmentation algorithms based on the datasets with sample cross-sections depicted in Figs. 6c and 6f. The tested algorithms included K-Means Clustering, Fuzzy C-Means Clustering, a Gaussian Mixture Model (GMM) (*Everitt et al., 2011*), and the Markov Random Field (MRF) algorithm developed by *Kulkarni et al. (2012)* (Fig. 7). Note that Fuzzy C-Means Clustering did not yield feasible results; hence was excluded from the comparison below.**
- **Segmentation results were compared with the exact data via the misclassification error (Table 1) defined as:**

$$\varepsilon = \frac{Number\ of\ Misclassified\ Voxels}{Total\ No.\ of\ Sample\ Voxels} \times 100$$

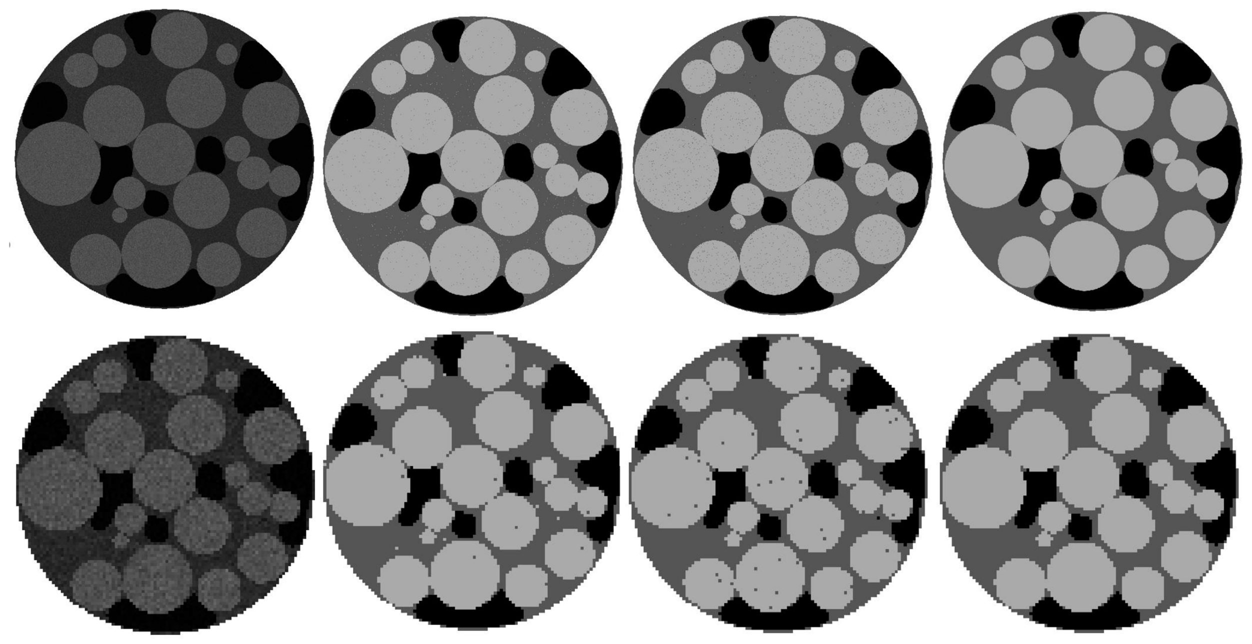

Figure 7: From left to right, data with added noise, GMM segmentation, K-Means segmentation, and MRF segmentation. Top row depicts data at 800×800 resolution and bottom row shows data at 100×100 resolution.

Table 1: Misclassification error of applied multiphase segmentation algorithms (Fuzzy C-Means Clustering did not yield feasible results, hence was excluded from the comparison).

	GMM	K-Means	MRF
ε (800×800)	0.4718	0.8676	0.0075
ε (100×100)	0.4708	0.8633	0.0271

Conclusions and Ongoing Work

- **Discrete Element Modeling (DEM) in conjunction with lattice Boltzmann (LB) simulations provides a powerful means for the synthesis of realistic three-phase porous media that after introduction of CT scanning artifacts can be used as reference for performance evaluation of binarization and multiphase segmentation algorithms.**
- **Comparison of 4 multiphase segmentation codes revealed that algorithms that account for the local voxel neighborhood perform better than algorithms relying on the global grayscale distribution.**
- **The presented study is a first step towards generation of realistic data for testing and refinement of segmentation techniques. Ongoing work includes DEM and LB simulations with particles exhibiting random irregular shapes to better mimic natural soils. Another objective of ongoing efforts is the implementation of additional CT acquisition artifacts.**

References

Everitt, B.S., S. Landau, M. Leese, and D. Stahl, 2011. "Cluster Analysis", 5th Edition, John Wiley & Sons, Chichester, UK.

Hsieh, J., 2009. Computed tomography: principles, design, artifacts, and recent advances. Bellingham, WA, SPIE.

Iltis, G.C., R.T. Armstrong, D.P. Jansik, B.D. Wood, and D. Wildenschild, 2011. Imaging biofilm architecture within porous media using synchrotron-based X-ray computed microtomography. Water Resour. Res., 47, W02601.

Kulkarni, R., M. Tuller, W. Fink, and D. Wildenschild, 2012. Three-Dimensional Multiphase Segmentation of X-Ray CT Data of Porous Materials Using a Bayesian Markov Random Field Framework. Vadose Zone J., 11, doi:10.2136/vzj2011.0082.

Schaap, M.G., Porter, M.L., Christensen, B.S. and Wildenschild, D., 2007. Comparison of pressure-saturation characteristics derived from computed tomography and lattice Boltzmann simulations. Water Resour. Res., 43, W12S06.

Šmilauer, V., E. Catalano, B. Chareyre, S. Dorofeenko, J. Duriez, A. Gladky, J. Kozicki, C. Modenese, L. Scholtès, L. Sibille, J. Stránský, K. Thoeni, 2010. Yade Reference Documentation. In Yade Documentation (V. Šmilauer, ed.), The Yade Project , 1st ed. (http://yade-dem.org/doc/)